



Final report 19.12.2016

Solution deposited ZnO-based front contacts for CIGS solar cells

SWISS PROJECT WITHIN “NOVAZOLAR”
SOLAR-ERA NETWORK



Schweizerische Eidgenossenschaft
Confédération suisse
Confederazione Svizzera
Confederaziun svizra

Eidgenössisches Departement für
Umwelt, Verkehr, Energie und Kommunikation UVEK
Bundesamt für Energie BFE

Auftraggeber:

Bundesamt für Energie BFE
Forschungsprogramm Photovoltaik
CH-3003 Bern
www.bfe.admin.ch

Auftragnehmer:

Laboratory for Thin Films and Photovoltaics, Empa
Überlandstrasse 129,
CH-8600 Dübendorf
www.empa.ch/tfpv

Authors:

Dr. Jérôme Steinhauser, Empa, jerome.steinhauser@empa.ch
Peter Fuchs, Empa, peter.fuchs@empa.ch
Dr. Patrick Reinhard, Flisom, patrick.reinhard@flisom.ch
Dr. Yaroslav Romanyuk, Empa, yaroslav.romanyuk@empa.ch
Prof. Dr. Ayodhya N. Tiwari, Empa, ayodhya.tiwari@empa.ch

BFE-Bereichsleiter: Dr. Stefan Oberholzer

BFE-Programmleiter: Dr. Stefan Nowak

BFE-Project /Contract Number: NovaZolar, 8100073 / SI/501100-01

Für den Inhalt und die Schlussfolgerungen ist ausschliesslich der Autor dieses Berichts verantwortlich.

Outline

1. Abstract	2
2. Background	2
3. Goals	3
4. Methods	3
5. Results and discussions	5
6. National / international Cooperations	14
7. Conclusions and outlook	14
8. References	15

1. Abstract

The aim of the “NovaZolar” Swiss project within the European SOLAR-ERA.NET program was to develop an innovative, low-cost process of solution deposition of the ZnO-based transparent electrical contacts for CIGS solar cells and photovoltaic mini-modules. Together with solution-grown ZnS-based buffers that were investigated by German and French national sub-projects, the novelty was to employ a single deposition technique – chemical bath deposition – for producing the Cd-free window and buffer layers.

The solution process with post-deposition UV annealing yielded transparent and conductive ZnO layers with a sheet resistance of 20Ω for a thickness of $2.7 \mu\text{m}$. An absolute efficiency of 18.3 % was achieved with the solution-grown ZnO electrodes, on par with the sputtered reference. The conductive doped ZnO layers were directly grown on Zn(O,S) buffers achieving an efficiency of 16 %, proving the feasibility of manufacturing the buffer-TCO bilayer using a single solution technique. Finally, solution electrodes were successfully implemented into flexible CIGS cells on polymer substrates with efficiency up to 13.8 % and mini-modules of $5 \times 5 \text{ cm}^2$ were manufactured.

Insufficient homogeneity, the need of thicker layers and a rather long deposition time have been identified as main deficiencies of the developed process. As a consequence, immediate industrial implementation and scale-up of the current laboratory process is predicted to result in ca. 40% cost increase as compared to reference sputter process. As outlook, further research activities on solution electrodes should focus on accelerating the deposition rate as well as improving the long term stability of ZnO with capping layers or extrinsic dopants.

2. Background

The Cu(In,Ga)Se₂ (CIGS) thin film solar cell technology has made a steady progress within the last decade by raising the conversion efficiency to 22.6% on laboratory scale [1], thus exceeding the highest efficiency for polycrystalline silicon cells [2]. Champion CIGS modules achieve efficiencies of up to 17.9% as mini-modules [3] or 16.5% for standard size [4], whereas commercially available CIGS modules are typically 12-14% efficient [5]. A state-of-art CIGS solar cell has the configuration sub-



strate/Mo contact/CIGS absorber/CdS buffer/i-ZnO/Al:ZnO window/metal grid. The CdS buffer layer is deposited by chemical bath deposition (CBD), and the transparent conductive oxide (TCO) layer of i-ZnO/Al:ZnO is deposited by vacuum sputtering. Both the CdS buffer and sputtered TCO layer are considered as bottlenecks of the current CIGS technology because of environmental concerns and the need of expensive vacuum equipment, respectively. A novel solution approach for highly conductive ZnO:Al without the need of conducting substrate has recently been disclosed by Empa and the first application of the AZO layers as TCOs in CIGS cells showed a promising efficiency of 14.8% at the project start [6].

3. Goals

The overall project goal was to develop a combination of Cd-free buffer and TCO material by scalable solution processing which would translate in the reduction of CIGS module costs, lower the equipment complexity, and increase material utilization. The buffer-TCO combination is realized on one material – ZnO – where the Zn(S,O) buffer will be followed by a solution deposited ZnO:Al TCO contact. The Swiss sub-project of Empa and Flisom AG was focused on the solution deposition of the ZnO-based transparent front contact for in CIGS cells and modules.

4. Methods

Chemical bath deposition of transparent and conductive doped ZnO

Chemical bath deposited Al-doped ZnO (CBD AZO) layers are grown on a seed layer (i-ZnO, 50 nm, sputtered on borosilicate glass) from an aqueous ammonia solution saturated with ZnO and heated at around 90 °C. The solution also contains ammonium citrate as a structure directing agent and ammonium nitrate as a buffer [6]. Aluminum is incorporated into the film as a dopant by her from dissolving aluminum nitrate in the deposition solution or by gradually adding a solution of ammonium citrate and aluminum nitrate during the deposition [7]. The layers are then exposed to UV radiation (Hg lamp with UVA, ~50 mW/cm²) for 10 minutes.

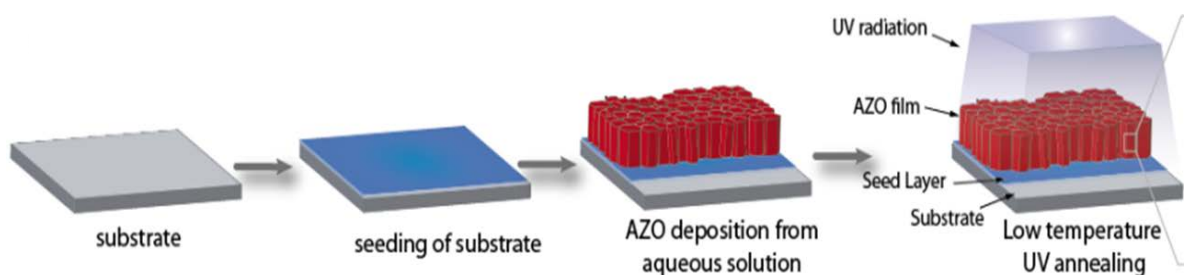


Fig. 1: Processing sequence of CBD AZO layers

Sputtered Al-doped ZnO reference electrodes

For cells with sputtered TCO, prior to the ZnO:Al TCO coating, the cell was coated with 80 nm of sputtered undoped zinc oxide in the case of cells with CdS buffer or with zinc magnesium oxide in the case of cells with Zn(O,S) buffers. RF magnetron sputtered AZO layers were deposited without intentional substrate heating in a vacuum chamber with a direct facing target. Ceramic ZnO:Al₂O₃ (98:2 wt%, purity 99.995%) targets with a diameter of 10.16 cm (4 in.) were sputtered in a mixed Ar/O₂ atmosphere with a total pressure of 0.15 Pa and a power density of 2.5 W.cm⁻².

Solar cells fabrication

CIGS absorber layer on molybdenum coated glass was deposited by an evaporation process combined with an alkali post-deposition treatment (PDT) [8, 9] or was inline deposited by a dynamic multistep process without an additional PDT [10]. CdS and Zn(O,S) buffer layer growth was performed by CBD [11]. CIGS absorber layers were deposited on flexible PI by elemental co-evaporation [12]. After TCO deposition, 50/4000/50 nm thick Ni/Al/Ni grids were deposited by e-beam evaporation. The cells were defined to a square of ~36 mm² by mechanical scribing. Selected cells were coated with evaporated MgF₂ antireflection coating (ARC). Figure 2 shows a picture of a 5x5 cm² sample with the cell geometry used in this project.



Fig. 2: Picture of a 5x5 cm² sample. Individual cells are 36 mm².

Characterization

The sheet resistance of the ZnO thin films was measured by a four-probe method with a Nagy meter SD-600. Hall measurements were conducted with an Ecopia HMS 3000 setup at room temperature in the dark using a van der Pauw contact geometry. Transmittance measurements were performed with a Shimadzu UV-3600 spectrophotometer with an integrating sphere. Transmittance values were measured with the glass substrate stack against air reference. External quantum efficiency (EQE) of solar cells was measured with a lock-in amplifier. A chopped white light source (900 W, halogen lamp, 360 Hz) and a dual grating monochromator generated the probing beam. The beam size was adjusted such that the illumination area was smaller than the device area. A certified monocrystalline silicon solar cell from Fraunhofer ISE was used as the reference cell. Cell temperature was controlled at 25°C with Peltier cooling and white light bias was applied. J–V characteristics of solar cells were measured under simulated standard-test conditions (25°C, 1,000 W.m⁻², AM 1.5 G illumination) in a sun-simulator with a HMI light source. A Keithley 2400 source meter with four-terminal sensing was used to acquire J–V characteristics.



5. Results and discussions

CBD ZnO properties

After optimization of the solution temperature, chemistry and deposition time, CBD ZnO layers were grown on seeded glass substrates, showing a sheet resistance of $20 \Omega_{\text{square}}$ for a thickness of $2.7 \mu\text{m}$ resulting in a resistivity of $5.2 \cdot 10^{-3} \Omega \cdot \text{cm}$ with a mobility of $10 \text{ cm}^2 \cdot \text{V}^{-1} \cdot \text{s}^{-1}$ and a carrier density of $1.2 \cdot 10^{20} \text{ cm}^{-3}$. Table 1 summarizes the properties and deposition parameters of doped and undoped CBD ZnO baseline established as baseline during the project.

Table 1: CBD parameters and properties for doped and undoped CBD ZnO layers on $5 \times 5 \text{ cm}^2$ substrates.

<i>Deposition parameters</i>	AZO baseline	Undoped baseline	
Time	60	60	min
Temperature	90	93	°C
Solution volume	400	400	mL
Citrate concentration	1.25	3	mM
Doping solution $\text{Al}(\text{NO}_3)_3$ concentration	100	-	mM
Doping solution citrate concentration	50	-	mM
Doping gradient	190	-	$\mu\text{L} \cdot \text{min}^{-1}$
<i>Layer properties</i>			
Thickness	1200	2700	nm
Sheet resistance	48	20	Ω_{square}
Resistivity	$5.8 \cdot 10^{-3}$	$5.2 \cdot 10^{-3}$	$\Omega \cdot \text{cm}$
Free carrier density	$1.5 \cdot 10^{20}$	$1.2 \cdot 10^{20}$	cm^{-3}
Free carrier mobility	7	10	$\text{cm}^2 \cdot \text{V}^{-1} \cdot \text{sec}^{-1}$
Visible transmittance	>80	>80	%

SEM cross section of a typical CBD ZnO layer, as well as transmittance and electrical properties of undoped CBD ZnO layer deposited on glass as compared to a sputtered ZnO:Al are shown in Figure 3. The compact growth could be achieved by controlling the quantity of ammonium citrate in the deposition solution. Layers with the same deposition condition were implemented as front TCO in the different type of solar cells presented in the following sections.

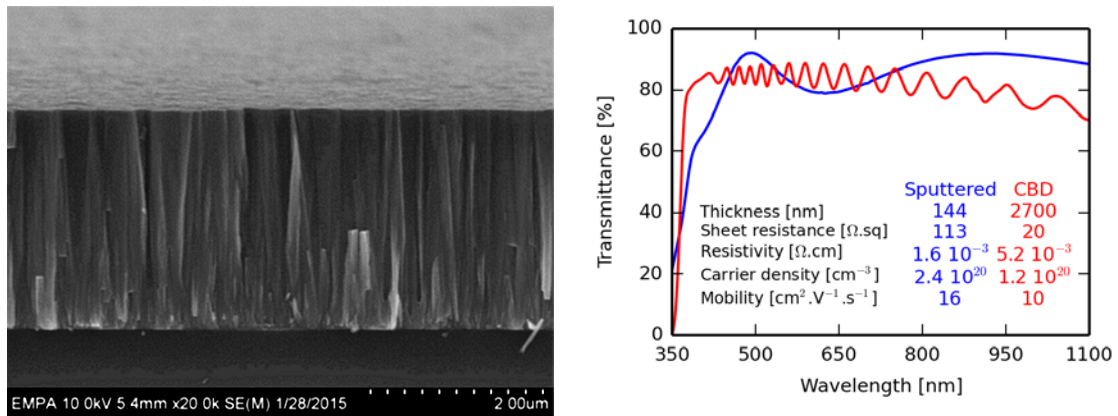


Fig. 3: (left) SEM micrograph cross section of a CBD ZnO layer deposited on glass. (right) Comparison of the transmittance and electrical properties of CBD ZnO with sputtered ZnO:Al deposited.

Solar cells with CdS buffer

Undoped CBD ZnO layers were implemented as front contact in CIGS solar cells with CdS buffer grown on glass substrates. Figure 4 shows SEM cross section of such a cell compared to a similar cell with a sputtered ZnO/ZnO:Al TCO.

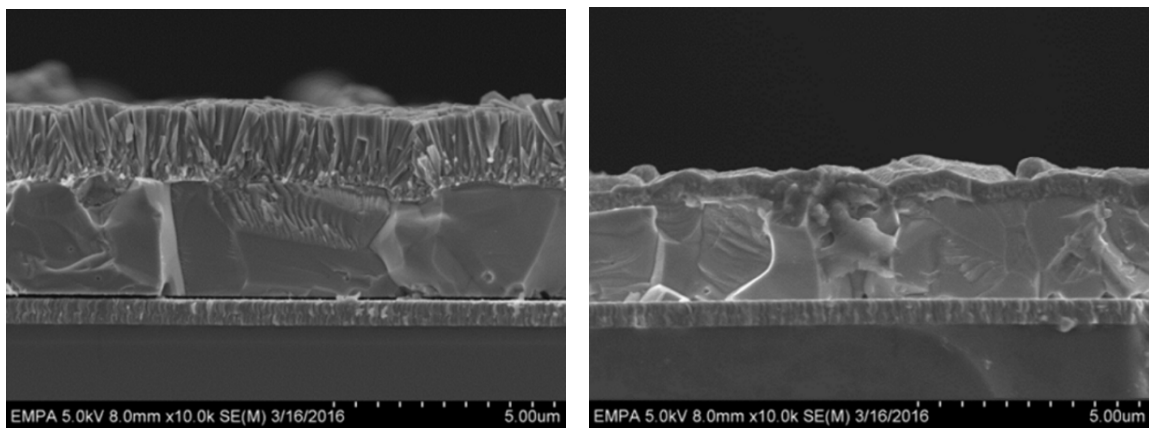


Fig. 4: SEM of cross section of cells with CBD ZnO layer (left) and with sputtered ZnO/ZnO:Al (right)

Figure 5 shows the properties of a set of CIGS/CdS solar cells with CBD ZnO and with sputtered ZnO/ZnO:Al as front TCO. The current densities are similar, but the fill factor and the open circuit voltage are slightly better with the sputtered contact compare to the CBD one. The lower open circuit voltage and fill factor for cells with CBD ZnO TCO is probably due to a more difficult cell scribing process in the case of the thicker CBD ZnO which can introduce shunts.

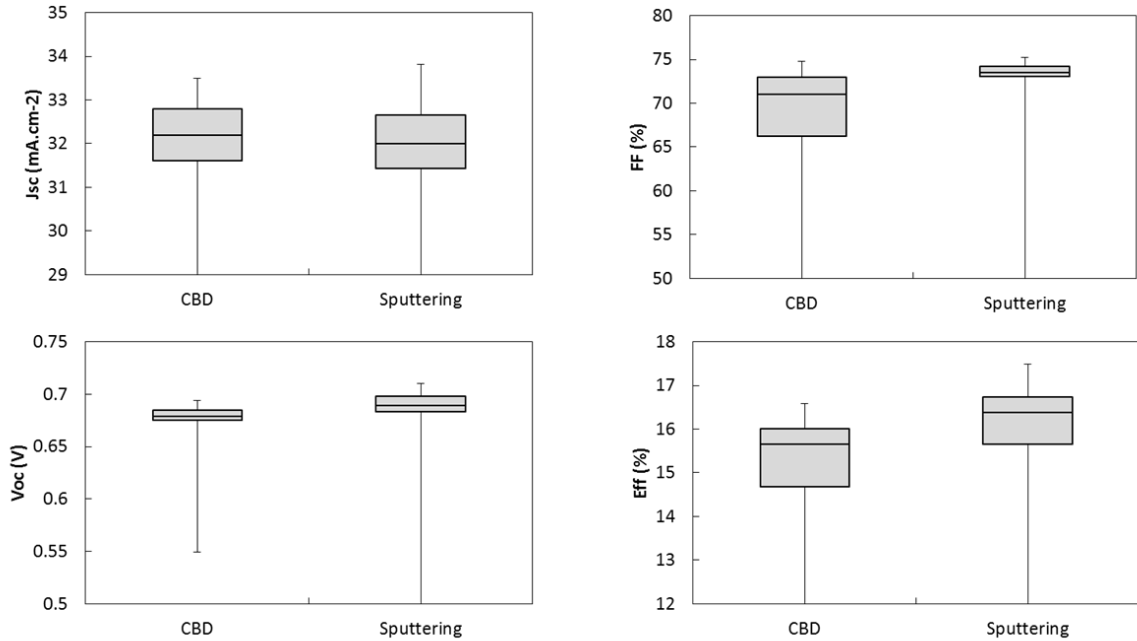


Fig. 5: Properties of a set of CIGS/CdS solar cells with CBD ZnO and with sputtered ZnO/ZnO:Al as front TCO

Figure 6 shows the current-voltage characteristics of the best cells together with their external quantum efficiency curves. With a CBD ZnO TCO, an efficiency of 16.6 % with a current density of 33.5 mA·cm⁻², an open circuit voltage of 674 mV and a fill factor of 73.8 % for a 0.36 cm² cell area are measured. This efficiency is close to 17.5 % obtained with sputtered ZnO:Al TCO on the same batch of CIGS cells.

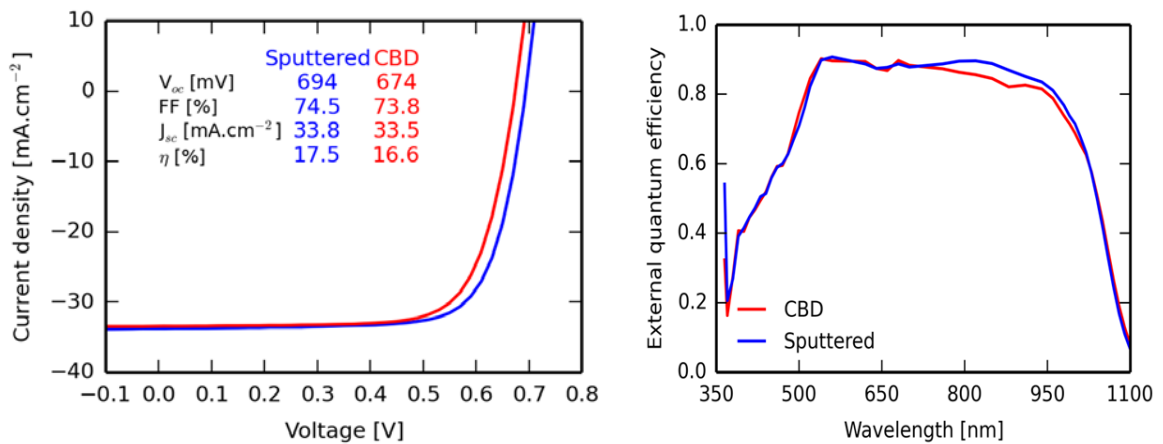


Fig. 6: (left) J-V characteristics and (right) EQE curves for the best CIGS/CdS solar cell with CBD ZnO and with sputtered ZnO/ZnO:Al as front TCO.

Solar cells with CdS buffer on flexible substrate

CBD ZnO layers were also implemented as front contact in CIGS solar cells with CdS buffer grown on flexible polyimide absorber. Figure 7 shows the SEM cross section of such cell. In this case an efficiency of 13.8 % was achieved with a V_{oc} of 644 mV, a FF of 67.6 % and a J_{sc} of 31.8 mA. These values are comparable with results of solar cells obtained with similar absorber with sputtered ZnO TCO and show that CBD ZnO TCO are compatible with flexible polyimide substrates.

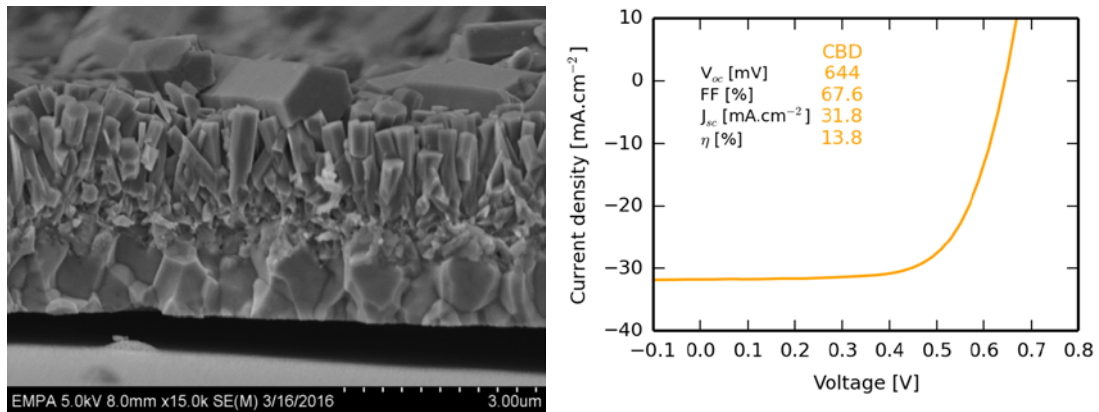


Fig. 7: (left) SEM of cross section of cells with CBD ZnO layer on PI substrat. (right) J-V characteristics of the best 36 mm² CIGS/CdS solar cell on flexible substrate with CBD ZnO.

Solar cells with Zn(O,S) buffer

Finally CBD ZnO was implemented as TCO in cells with solution-grown Zn(O,S) buffer layer on glass substrates in order to demonstrate the feasibility to realize the buffer-TCO stack with a single deposition technique. The absorbers were provided by ZSW partners (Germany) and are comparable with the one used in section 4.1 with CdS buffers.

Solar cell properties of CIGS/CdS solar cells with CBD ZnO and with sputtered ZnO/ZnO:Al as front TCO are depicted in Figure 8. The current densities is lower for cells with sputtering contact, this is presumably due to interference fringes in the ZnMgO. The fill factor and the open circuit voltage are comparable.

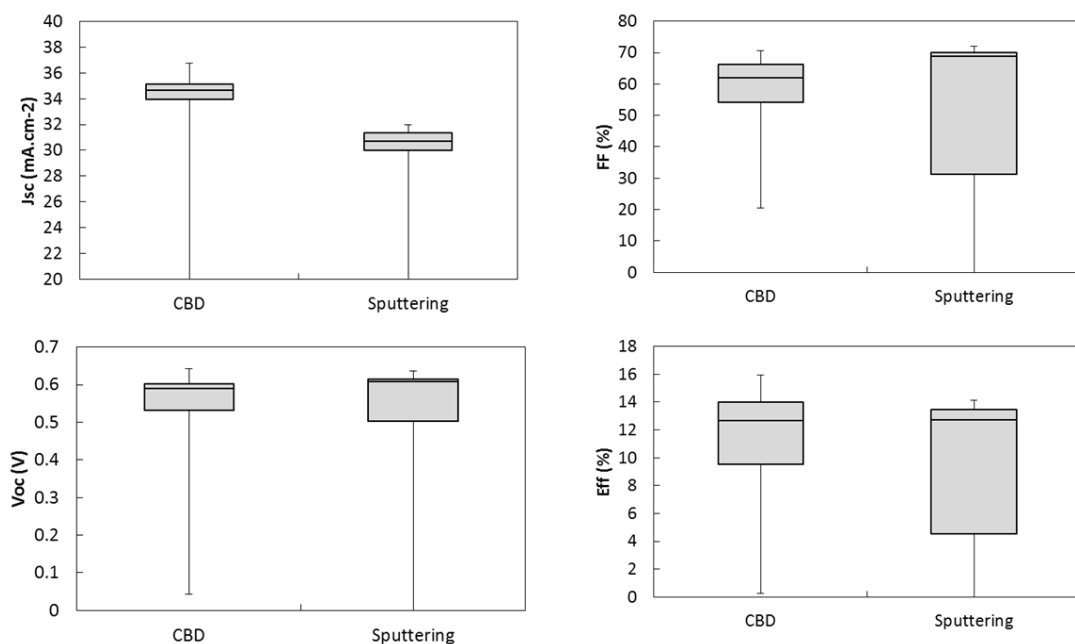




Fig. 8: Properties of a set of CIGS/Zn(O,S) solar cells with CBD ZnO and with sputtered ZnO/ZnO:Al as front TCO

Figure 9 shows the current-voltage characteristics of the best cell with CBD TCO. We achieved an efficiency of 16 % with a current density of 35.2 mA cm^{-2} , an open circuit voltage of 642 mV and a fill factor of 70.6 % for a 0.36 cm^2 cell area. With this result realized a cell with cadmium-free fully solution processed window (buffer and TCO) is demonstrated.

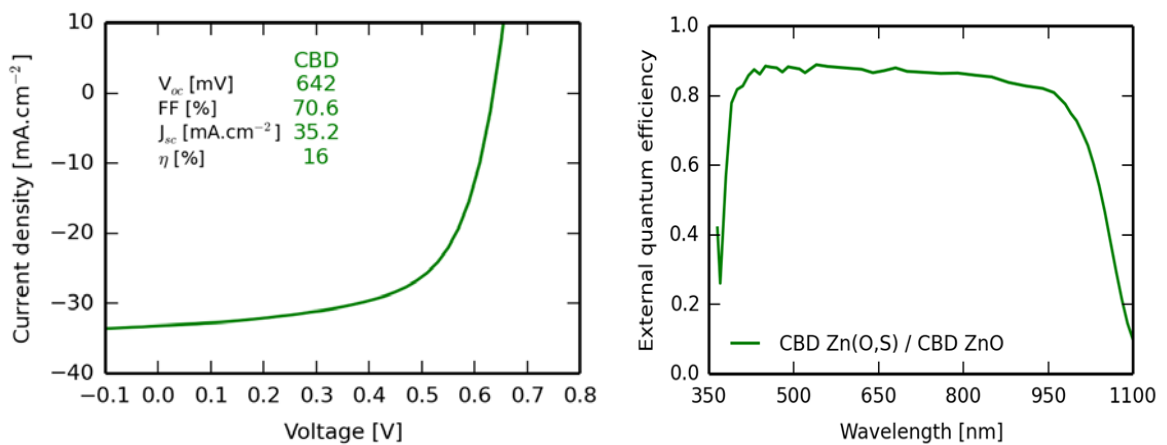


Fig. 9: (left) J-V characteristics and (right) EQE curve of the best CIGS/Zn(O,S)/ZnO solar cell.

Mini modules implementation

Mini-modules were fabricated with CBD ZnO as contact layer. The mini-modules consist of 8 elementary cells monolithically connected in series using laser scribing done at Flisom on $5 \times 5 \text{ cm}^2$ on polyimide (PI) substrates. Figure 10 shows a picture of the mini-module together with the current-voltage characteristics of a working mini-module. An efficiency of 5.05 % with a current of 29.65 mA was measured along with an open circuit voltage of 4.3 V and a fill factor of 40.5 % for a 10.24 cm^2 total area.

The fact that mini-module performance was lower than that for a reference with sputtered AZO contact can be attributed to the fact that laser scribing parameters have to be thoroughly optimized for the thick CBD AZO contact. Still, the working flexible mini-module is a proof-of-concept and a clear advancement over the state of art.

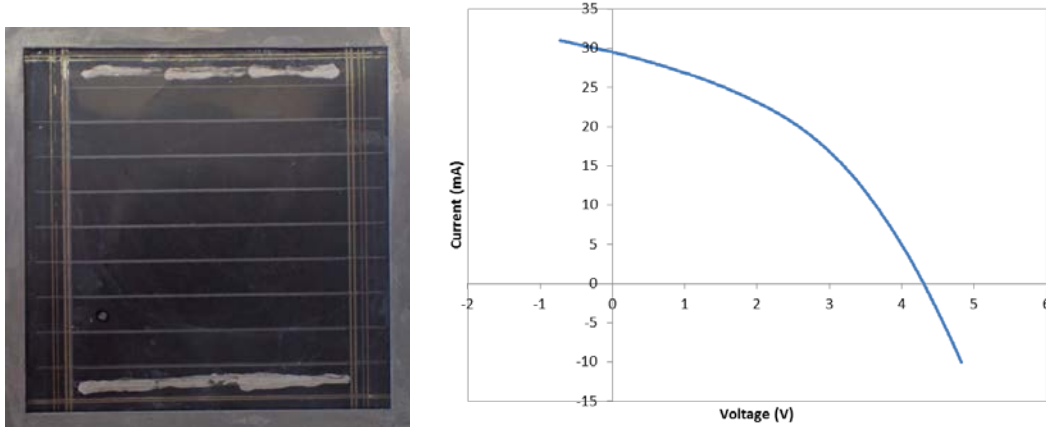


Fig. 10: (left) Photo and (right) I-V characteristics of the 5x5 cm² flexible mini-module with ZnO CBD.

Deliverable 3.1: cell with efficiency over 20%

CBD ZnO layers were finally implemented as front contact on evaporated CIGS absorber with CdS buffer on glass substrate (obtained from ZSW partners) in order to reach the highest possible absolute cell efficiency. Figure 11 shows the properties of a set of high efficiency CIGS/CdS solar cells with CBD ZnO and with sputtered ZnO/ZnO:Al as front TCO. MgF₂ antireflection coating was applied. The current densities and open circuit voltage are similar; the fill factor is slightly better with the sputtered contact compare to the CBD one. The lower open circuit voltage and fill factor for cells with CBD ZnO TCO is probably due to a more difficult cell scribing process in the case of the thicker CBD ZnO which can introduce shunts. Figure 12 shows the current-voltage characteristics of the best cell achieved: 18.3 % efficiency with a Voc of 703 mV, a FF of 70.4 % and a Jsc of 37 mA.

The efficiency of 18.3% is equal to the efficiency of 18.3% obtained for the sputtered i-ZnO-AZO bi-layer but still significantly lower than 19.3% (without ARC coating) measured on fresh reference cells at ZSW prior to shipping absorbers to Empa. Even though the milestone of 20% could not be reached, it is shown that solution-processed TCOs can yield absolute peak efficiencies comparable to the sputtered references. The uniformity and reproducibility of the solution-processed TCO are still inferior as can be seen from larger statistical spreads in Figure 11.

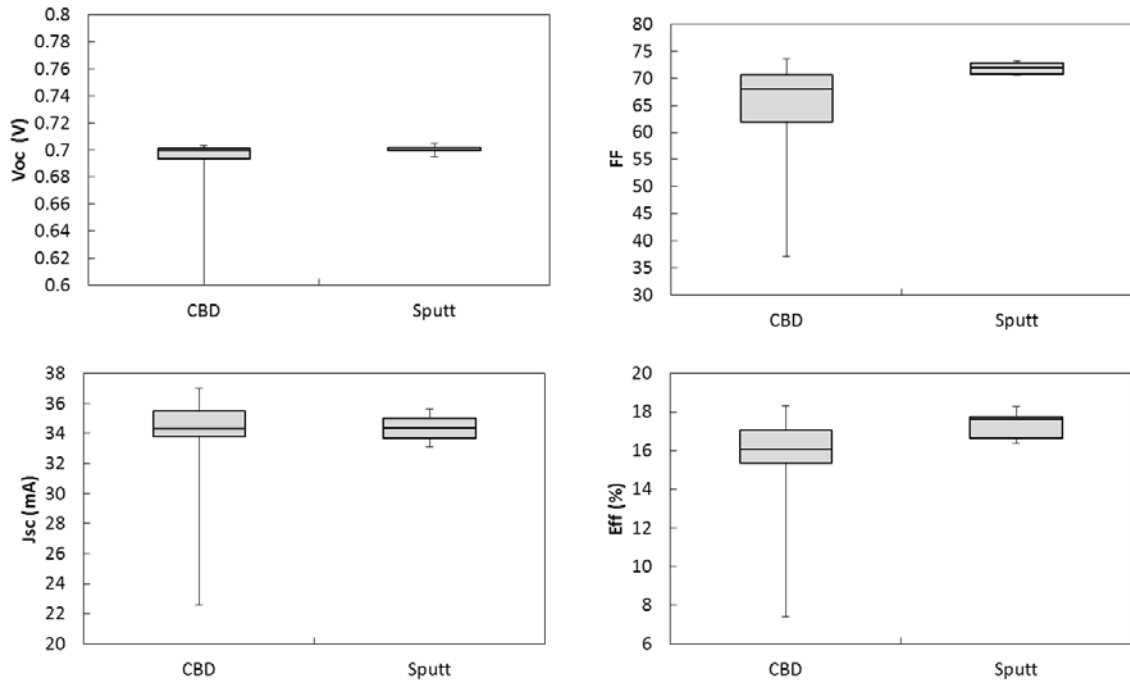


Fig. 11: Properties of a set of high efficiency CIGS/CdS solar cells with CBD ZnO and with sputtered ZnO/ZnO:Al as front TCO

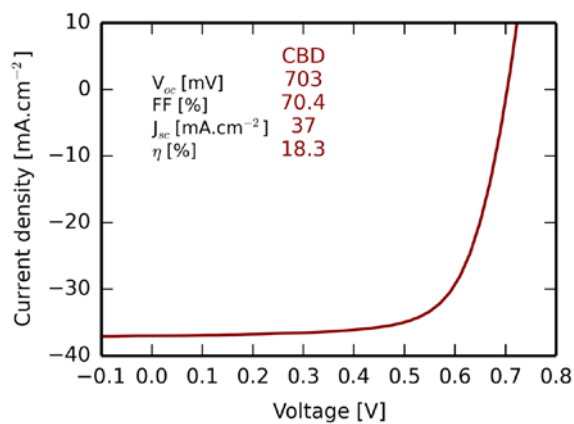


Fig. 12: J-V characteristics of the best 36 mm² CIGS/CdS solar cell with CBD ZnO and AR coating.

Deliverable 6.1: Cost analysis of expected CAPEX and OPEX for solution TCO as compared to sputtered one (Flisom).

In this deliverable, the cost of solution TCO is compared to the cost of sputtered TCO. The analysis was performed using the deposition parameters used on lab-scale for solution TCO, and compared to the cost of R2R sputtered TCO currently applied on industrial scale by Flisom. Deposition of solution

TCO on industrial scale is assumed to be done on same type of hardware equipment as currently done for solution CdS, without the need for any major modifications.

Cost calculations were made assuming 100 MW Fab, producing 1 m² modules of 140 W on a web width of 1 m (total area efficiency of modules at 14%). Depreciation time for the hardware is set at 5 years. Consumables and maintenance costs are assumed at 2%, resp. 5% of hardware cost. Labor cost is similar for both processes, because the coated area remains the same for both TCO deposition approaches. Energy consumption for CBD machines is considered equal, and the minor difference that could arise from the higher bath temperature required for solution TCO compared to solution CdS is neglected. We furthermore assume same efficiency for both TCO approaches.

The thickness of the sputtered TCO is 1100 nm (100 nm i-ZnO and 1000 nm ZnO:Al), whereas the thickness of solution TCO is 2700 nm. Using R2R CBD deposition tool, standard deposition time for CdS layer is 10 min. For solution TCO, deposition time on laboratory scale is 60 min. Assuming that the process can be faster when optimizing for industrial scale (by change of solution chemistry or temperature, without significant impact on material costs), we aim at 30 min deposition time. Therefore, by using the same hardware for R2R solution TCO, we can expect that hardware costs are increased by a factor 3 for same throughput.

Figure 13 shows a comparison of relative total cost for CBD CdS, sputtered TCO and solution TCO. Cost for CBD CdS is set as reference. The higher cost of solution TCO compared to CBD CdS comes from the fact that the solution TCO requires much longer deposition times, therefore higher investments costs when using similar equipment. With this scenario, solution TCO is 40% more expensive than sputtered TCO, and therefore solutions are required to reduce its cost in order to make it competitive on industrial scale.

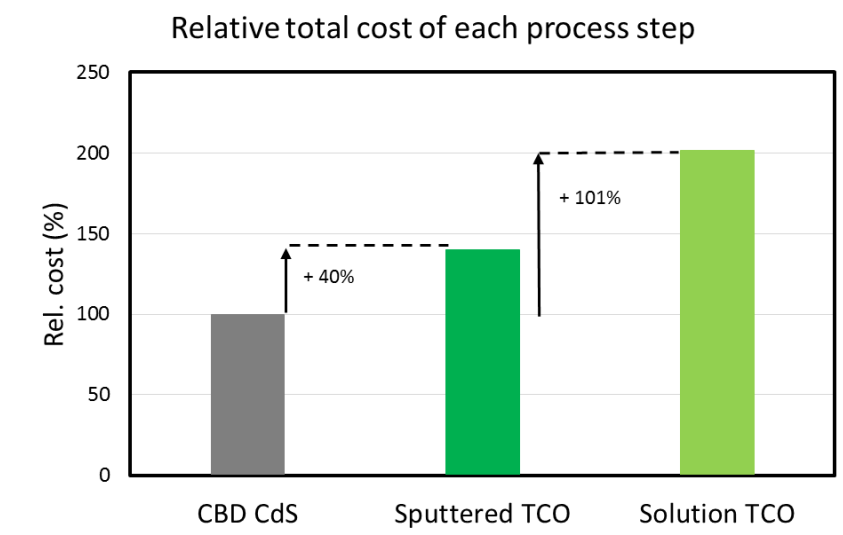


Fig.13: Relative total cost of CBD CdS, sputtered TCO and solution TCO.

Figure 14 shows the cost structure of sputtered TCO and solution TCO, compared to CBD CdS. In all cases, depreciation and material costs account for about 65-70%. Facility, energy, maintenance, labour and consumables represent only a smaller proportion of the total cost. This shows that the different scenarios are not to be significantly affected by choosing more precise assumptions than those discussed above for those aspects. Capital investments for hardware are the main factors that prevent solution TCO from having lower CAPEX and OPEX than sputtered TCO.

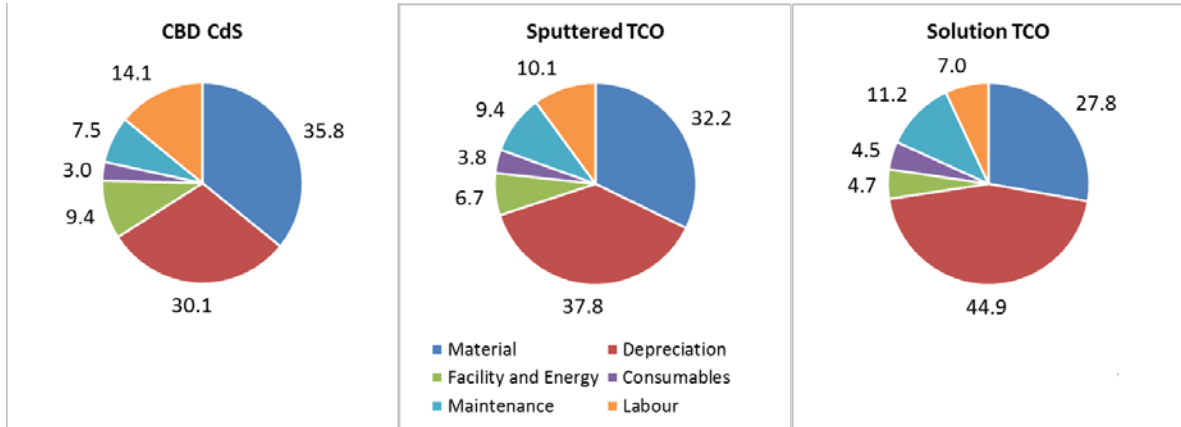


Fig.14: Relative total cost of CBD CdS, sputtered TCO and solution TCO.

Different strategies can be pursued in order to reduce the cost of solution TCO. On one hand, reduction of equipment cost could be expected by developing a much faster TCO deposition rate recipe that should allow depositing the TCO layer in a similar time as CdS (i.e. 10 min). This would thereby reduce the number of coaters required to have same throughput as for CdS. In this hypothetical case, a reduction of operating costs of 15% could be expected for solution TCO compared to sputtered TCO, as shown in Figure 15.

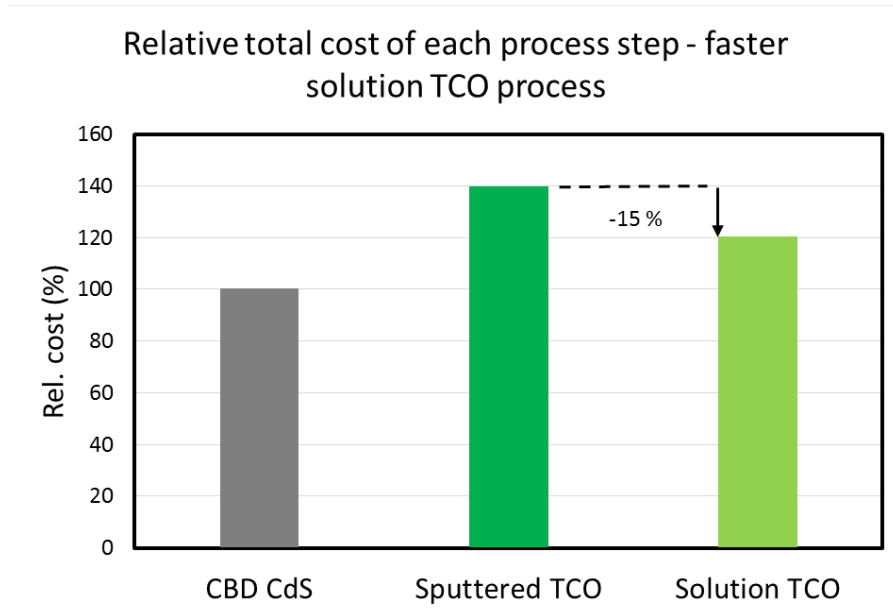


Fig. 15: Relative total cost of CBD CdS, sputtered TCO and solution TCO for the hypothetical scenario of the fast solution growth (growth time 5 min).

Another important consideration is raw material costs. Figure 16 shows the share of the different materials used for deposition of the TCO. Zinc oxide, ammonium nitrate and ammonium citrate have the largest share and significant reduction of total cost could be expected either by lowering their usage, or finding suitable alternatives at lower price. This might also be the result of development of

a faster deposition recipe with new complexants and precursors, or reduced amount of solution required for each deposition.

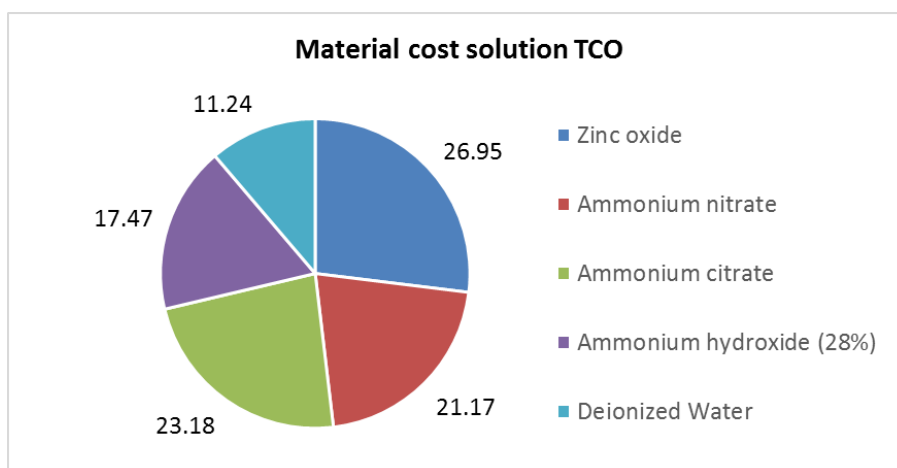


Fig. 16: Relative cost share of chemicals used for solution TCO.

In conclusion, the solution TCO approach using the extrapolated laboratory recipe is not a suitable alternative to sputtered TCO from the cost point of view at this moment. Development of a recipe to enable a faster deposition on par with sputtering can still be a viable alternative to sputtered TCO, provided that the module efficiency is identical (which is not the case as of today).

6. National / international Cooperations

The NovaZolar project within the SOLAR-ERA network foresees a close collaboration between all project partners:

EMPA - Swiss Federal Laboratories for Materials Science and Technology	Switzerland
Flisom AG	Switzerland
CNRS - Centre national de la recherche scientifique	France
EDF	France
NEXCIS	France
ZSW - Zentrum für Sonnenenergie- und Wasserstoff-Forschung	Germany
Manz CIGS Technology GmbH	Germany
IREC - Fundacio Privada Institut de Recerca en Energia de Catalunya	Spain

7. Conclusions and outlook

Solution-processed doped ZnO transparent contacts have been developed, and in cooperation with other NovaZolar partners successfully implemented into high-efficiency CIGS solar cells and mini-modules. Table 2 summarizes characteristics of best cells grown on different substrates:

- An absolute efficiency of 18.3 % was achieved with the solution-grown ZnO electrode, on par with the sputtered reference. Uniformity of the CBD TCO was however inferior to the sputtered reference.
- The CBD ZnO layers were directly grown on Zn(O,S) buffers achieving an efficiency of 16 %, which proves the feasibility of manufacturing the buffer-TCO bilayer using a single solution technique.



- CBD ZnO were successfully implemented on flexible PI substrates up to an efficiency of 13.8 %. Mini modules with an efficiency of 5% were also demonstrated. Scribing of mini-modules should be optimized and encapsulation is needed for long term stability.
- UV exposure is needed to improve electrical properties of CBD ZnO. The optimized wavelength was determined and is 360-365 nm, which ensures the above band-gap excitation and a deep enough penetration in the layer.
- Direct scale-up of the current process would result into a cost increase of about 40% compared to sputtered solution. This is primarily due to the larger thickness of CBD ZnO which requires a deposition time of 60 min.

Table 2: Summary of the best cells characteristics

Substrate	Absorber	Buffer	TCO	Voc (mV)	Jsc (mA.cm ⁻²)	FF (%)	Eff (%)
Glass	in-line CIGS ZSW	CdS	Sputt ZSW	694	33.8	74.5	17.5
Glass	in-line CIGS ZSW	CdS	Sputt empa	717	33.8	71.9	17.4
Glass	in-line CIGS ZSW	CdS	CBD ZnO	674	33.5	73.8	16.6
Glass	High quality CIGS ZSW	CdS	Sputt ZSW	683	36.5	77.4	19.3
Glass	High quality CIGS ZSW	CdS	Sputt empa + ARC	700	35.6	73.3	18.3
Glass	High quality CIGS ZSW	CdS	CBD ZnO +ARC	703	37	70.4	18.3
Glass	in-line CIGS ZSW	Zn(O,S)	Sputt ZSW	637	30.8	72.1	14.1
Glass	in-line CIGS ZSW	Zn(O,S)	Sputt empa	303	32.9	60.2	6
Glass	in-line CIGS ZSW	Zn(O,S)	CBD ZnO	642	35.2	70.6	16
PI	CIGS Flisom	CdS	CBD ZnO	644	31.8	67.6	13.8

As outlook, further research activities on CBD TCO should focus on the increase of the deposition rate as well as reduction of UV annealing time. The later could be tackled using high power UV flash annealing. For commercial implementation, improving long term stability of ZnO with capping layers or extrinsic dopants is also mandatory.

8. References

- [1] P. Jackson, R. Wuerz, D. Hariskos, E. Lotter, W. Witte, and M. Powalla, **Effectsof heavy alkali elements in Cu(In,Ga)Se2 solar cells with efficiencies up to 22.6 %**, Physica Status Solidi (RRL) 586 (2016).
- [2] M.A. Green, K. Emery, Y. Hishikawa, W. Warta, E.D. Dunlop, **Solar cell efficiency tables (version 44)**, Prog. Photovolt: Res. Appl. 22 (2014) 701-710.

- [3] Avancis press release, 02.05.2016, Torgau / München, <http://www.avancis.de/en/press/news/>
- [4] TSMC Solar Ltd. Press release, 28.04.2015, <http://www.tsmc-solar.com/>
- [5] PICON Solar, **Presentation at 4th Thin-film Industry Forum**, 2012, <http://www.picon-soar.de/download/Total%20cost%20of%20ownership%20for%20CIGS%20thin%20film%20PV%20module%20production.pdf>.
- [6] H. Hagendorfer, K. Lienau, S. Nishiwaki, C. M. Fella, L. Kranz, A. R. Uhl, D. Jaeger, L. Luo, C. Gretener, S. Buecheler, Y. E. Romanyuk, A. N. Tiwari, **Highly Transparent and Conductive ZnO:Al Thin Films from a Low Temperature Aqueous Solution Approach**, Adv. Mater. 26 (2014) 632-636.
- [7] P. Fuchs, H. Hagendorfer, Y. E. Romanyuk, A. N. Tiwari, **Doping strategies for highly conductive Al-doped ZnO films grown from aqueous solution**, Phys. Status Solidi A. doi: 10.1002/pssa.201431145 (2014).
- [8] P. Jackson, D. Hariskos, R. Wuerz, O. Kiowski, A. Bauer, T. M. Friedlmeier, and M. Powalla, Phys. Status Solidi RRL 9, No. 1, 28-31, 2015.
- [9] P. Jackson, D. Hariskos, R. Wuerz, W. Wischmann, and M. Powalla, Phys. Status Solidi RRL 8, No. 3, 219-222, 2014.
- [10] G. Voorwinden, R. Kniese, P. Jackson, M. Powalla, Proceedings of the 22nd European Photovoltaic Solar Energy Conference EU-VSEC, Milan, Italy, September 3-7, 2007, pp.2115-2118.
- [11] D. Hariskos, P. Jackson, W. Hempel, S. Paetel, S. Spiering, R. Menner, W. Wischmann, and M. Powalla, Proceedings of the 43rd IEEE Photovoltaic Specialists Conference, Portland USA, June 5-10, 2016.
- [12] A. Chirilă, P. Bloesch, S. Seyrling, A. Uhl, S. Buecheler, F. Pianezzi, C. Fella, J. Perrenoud, L. Kranz, R. Verm, D. Guettler, S. Nishiwaki, Y.E. Romanyuk, G. Bilger, D. Brémaud and A.N. Tiwari, Prog. Photovolt: Res. Appl., 19: 560-564. doi:10.1002/pip.1077, 2011.